

Temporal changes in the frequencies and widths of the solar p-mode oscillations

E J Rhodes, Jr^{1,2}, **J Reiter**³, **J Schou**⁴, **T Larson**⁴, **P Scherrer**⁴,
J Brooks¹, **P McFaddin**¹, **B Miller**¹, **J Rodriguez**¹, **J Yoo**¹

¹ Department of Physics & Astronomy, University of Southern California,
Los Angeles, CA 90089-1342, U.S.A.

² Space Physics Research Element, Jet Propulsion Laboratory, Pasadena, CA 91101, U.S.A.

³ Zentrum Mathematik, Technische Universität München, D-80333 Munich, Germany

⁴ HEPL 4085, Department of Physics, Stanford University, Stanford, CA 94305-4085, U.S.A.

E-mail: erhodes@usc.edu

Abstract. We present a study of the temporal changes in the sensitivities of the frequencies and widths of the solar p-mode oscillations to corresponding changes in the levels of solar activity during Solar Cycle 23. From MDI and GONG++ full-disk Dopplergram three-day time series obtained between 1996 and 2008 we have computed a total of 221 sets of m-averaged power spectra for spherical harmonic degrees ranging up to 1000. We have then fit these 221 sets of m-averaged power spectra using our WMLTP fitting code and both symmetric Lorentzian profiles for the peaks as well as the asymmetric profile of Nigam and Kosovichev to obtain 442 tables of p-mode parameters. We then inter-compared these 442 tables which comprise in excess of 5.3 million p-mode parameters, and we performed linear regression analyses of the differences in p-mode frequencies and widths as functions of the differences in as many as ten different solar activity indices. From these linear regression analyses we have discovered new signatures of the frequency shifts of the p-modes and a similar, but slightly different, signature of the temporal shifts in the widths of the oscillations.

1. Introduction

At the present time, there is still disagreement over the nature of the physical mechanism which causes the frequencies of the solar p-mode oscillations to change during each solar cycle. Our main motivation for this study was our desire to provide more-detailed evidence of the frequency dependence of the responses of the oscillation frequencies to changes in solar activity than has been available in the past. Our hope has been that we could provide additional constraints on the possible mechanism that causes these frequency shifts.

2. Results

From MDI and GONG++ full-disk Dopplergram three-day time series obtained between 1996 and 2008 we have computed a total of 221 sets of m-averaged power spectra for spherical harmonic degrees ranging up to 1000. We have then fit these 221 sets of m-averaged power spectra (193 sets from MDI observations and 28 sets from GONG++ observations) using our WMLTP fitting code (Rhodes et al., 2001; Reiter et al., 2002) and both symmetric Lorentzian profiles for the peaks as well as the asymmetric profile of Nigam and Kosovichev (1998) to obtain

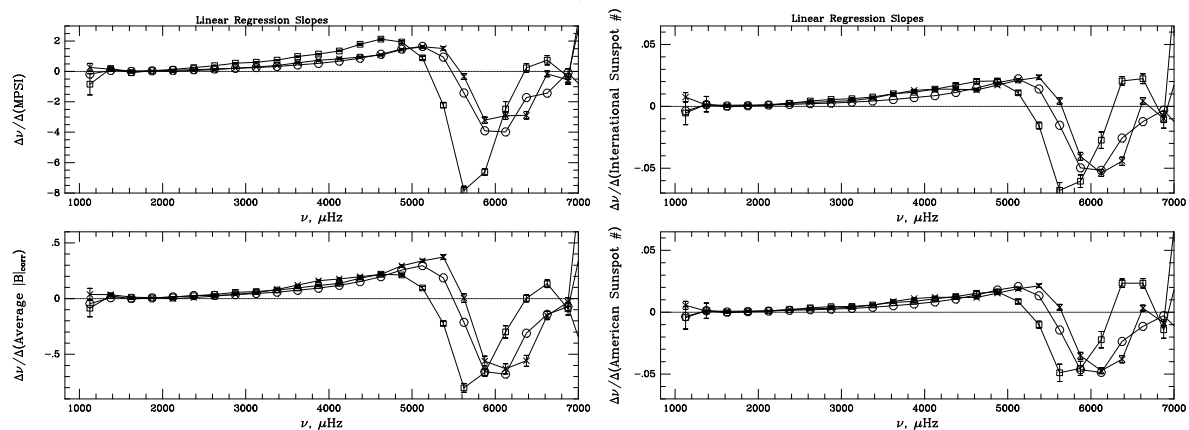


Figure 1. a.(top-left) The frequency dependence of the slopes of 75 separate linear regression analyses of symmetric-fit p-mode frequency shifts (which were binned in $250 \mu\text{Hz}$ -wide bins) upon differences in Magnetic Plage Strength Index, MPSI. The late-2001 GONG+ (solar maximum) results are shown as the Xs, while the 1996 MDI (solar minimum) results are shown as the squares, and the early-2001 MDI results are shown as the circles. The average level of activity during the 2001 MDI time interval was slightly below that of the GONG++ time interval. The three \pm zero-crossing frequencies can be seen to have increased systematically with increasing solar activity. Similarly, the three \mp zero-crossing frequencies also increased systematically between 1996 and late 2001, as can be seen at the far right side of the panel. b.(lower-left) The frequency dependence of the 75 sets of linear regression slopes for which changes in the average of the unsigned magnitude of the corrected photospheric magnetic field, $|B|_{\text{corr}}$, served as the independent variable. c.(top-right) Same as in panels a and b except that here differences in the three-day averages of the International Sunspot Number were used as the independent variable in the regression analyses. d.(bottom-right) In this case, differences in the three-day averages of the American Sunspot Number were used as the independent variable.

442 tables of p-mode parameters. We then inter-compared these 442 tables which comprise in excess of 5.3 million p-mode parameters, and we performed linear regression analyses of the differences in p-mode frequencies, widths, amplitudes, and asymmetries as functions of the differences in as many as ten different solar activity indices. Examples of the frequency dependence of some of the slopes of these linear regression comparisons are shown here in Figure 1. In Figure 1a, we show the frequency dependence of the 25 different slopes which we obtained from the linear regression analyses of the GONG++ frequency shifts upon the differences in the Magnetic Plage Strength Indicator (MPSI) as the Xs, while the 25 similar MDI regression slopes from early-2001 are shown as the circles, and 25 additional regression slopes computed from MDI observations obtained during 1996 are shown as the squares. In this panel we can see that the regression slopes did in fact change sign at three different frequencies in the case of the GONG++ and the two sets of MDI analyses. Based upon these results, we have defined the frequency at which the sign of the regression slopes change from being positive to being negative as the \pm zero-crossing frequency. Figure 1a also shows that both sets of regression slopes later changed sign again from negative to positive at much higher frequencies. We refer to the locations of these changes in sign as the \mp zero-crossing frequencies. In fact, both the \pm and the \mp zero-crossing frequencies were shifted toward higher values for the GONG++ observations from solar maximum in comparison with the zero-crossing frequencies of the MDI observations from solar minimum conditions. We believe that the most intriguing new feature that can be seen in Figure 1a is the obvious displacement of the two 2001 curves (i.e., the Xs and the circles) toward the right side of the panel. The location where the frequency

shifts change sign from positive to negative was moved to a higher frequency when the level of solar activity increased from the minimum levels of 1996 to the intermediate levels of early-2001 and was shifted even higher when the level of activity was the highest in late-2001. To our knowledge, this frequency shift in the zero-crossing frequency of the temporal frequency shifts has never been seen before by any other helioseismology studies. Not only are the zero-crossing frequencies shifted toward higher frequencies with increasing activity, but the entire high-frequency portions of the GONG++ and the 2001 MDI curves are shifted toward the right side of the plot. The same behavior can be seen in Figure 1b where the independent variable used in the regression analyses was the difference in average value of the unsigned magnitude of the corrected photospheric magnetic field, $|B|_{\text{corr}}$. The same behavior can also be seen in Figures 1c and 1d, where we have plotted the regression slopes which we obtained when we employed the differences in the International and American Sunspot Numbers as the independent variables, respectively.

In Figure 2a we show the dependence of both the \pm and \mp zero-crossing frequencies upon the average International Sunspot Number of each of the 16 time intervals. These zero-crossing frequencies were all computed using symmetric Lorentzian profiles. In Figure 2b we show the similar solar cycle dependence of both sets of zero-crossing frequencies which we computed using the asymmetric profile of Nigam and Kosovichev (1998). Both of these panels show that the frequency where the temporal frequency shifts change from being correlated to being anti-correlated with solar activity changes with the mean level of activity. Both panels also show that the frequency at which the frequency shifts go back to being positively correlated with the activity changes also changes with the mean level of activity.

In addition to studying the sensitivity of the temporal frequency shifts to changes in solar

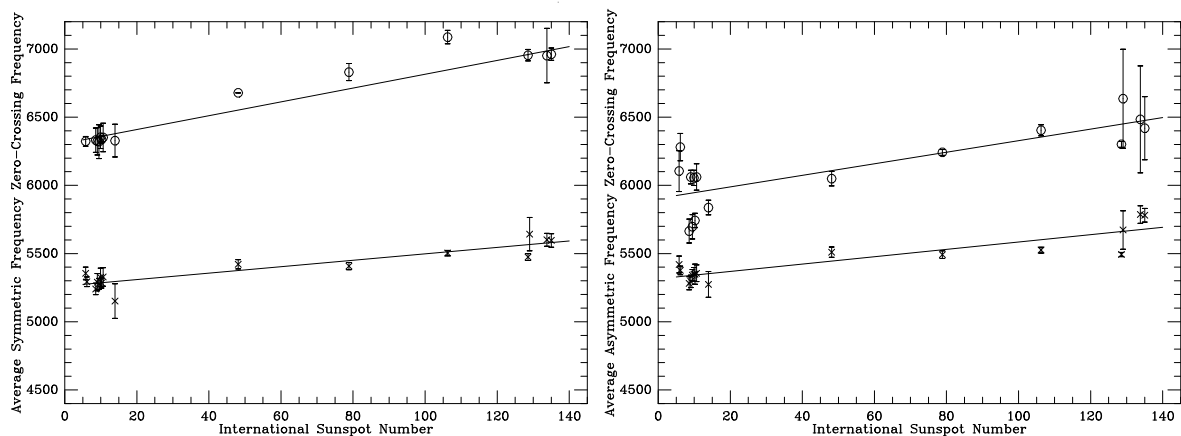


Figure 2. a.(left) Dependence of the mean \pm zero-crossing frequencies (the xs) for all 16 different time intervals upon the mean value of the International Sunspot Number during each of those 16 time periods. The straight line is the linear regression fit to the 16 data points. It shows that the differences in the zero-crossing frequencies which were evident in all four panels of Figure 1 were three different examples of the solar cycle dependence of those zero-crossing frequencies. The 16 corresponding mean \mp zero-crossing frequencies are shown as the 16 open circles in the upper portion of the panel. The linear regression fit to the 16 mean \mp zero-crossing frequencies is shown as the upper solid line. b.(right) Similar results to those shown in the left-hand panel except that the asymmetric fitting profiles were used instead of the symmetric Lorentzian profiles. The \pm zero-crossing frequencies and regression line were very similar to the results obtained using the symmetric profiles. However, the 15 \mp zero-crossing frequencies computed using the asymmetric profiles were systematically lower than the corresponding points in panel a.

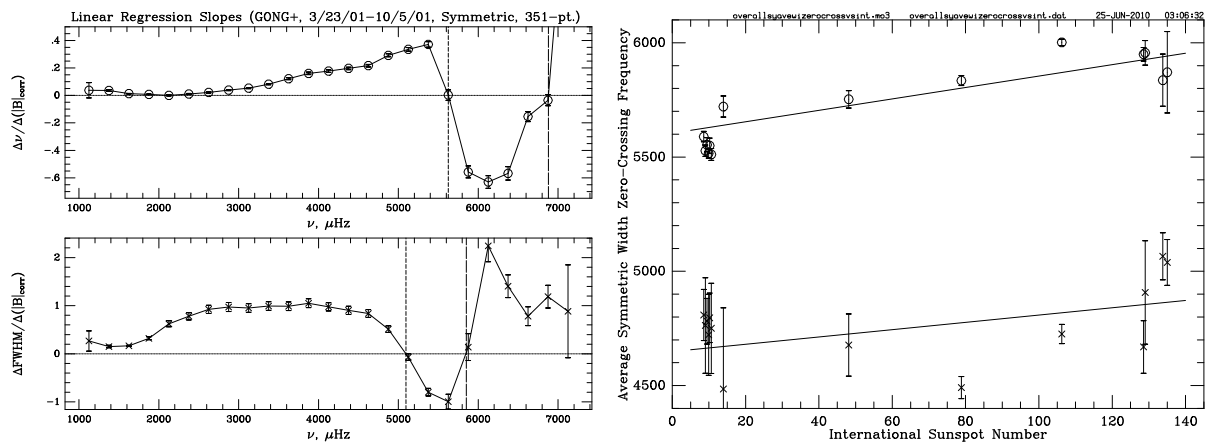


Figure 3. a.(upper-left) The frequency dependence of the 25 linear regression slopes from our study of the frequency shifts in which differences in the $|B|_{\text{corr}}$ served as the independent variable. The \pm zero-crossing frequency is marked by the vertical short-dashed line located near $5625 \mu\text{Hz}$, while the corresponding \mp zero-crossing frequency is shown by the long-dashed line at the far right edge of the panel. b.(lower-left) Frequency dependence of the 25 linear regression slopes from our study of the width shifts using the same independent variable. The two zero-crossing frequencies are again marked with similar dashed lines near $5100 \mu\text{Hz}$ and $5800 \mu\text{Hz}$, respectively. It is clear that both of these zero-crossings are located at lower frequencies than are the corresponding zero-crossings for the frequency shifts. c.(right) Dependence of both the \pm and \mp zero-crossing frequencies upon the mean levels of the International Sunspot Number as computed from our study of the temporal shifts of the p-mode widths. The lower solid line is the linear regression fit to the 16 \pm zero-crossing frequencies. The upper solid line is the linear regression fit to the 16 \mp zero-crossing frequencies. The slopes of these two regression fits are similar to, but somewhat smaller than, the slopes of similar regression fits that we obtained from our sensitivity analyses of the temporal frequency shifts.

activity, we repeated all of our regression analyses with the temporal shifts in the full-width-at-half-maxima (FWHM) taking the place of the temporal shifts in the frequencies. In Figure 3 we show the frequency dependences of the linear regression slopes that we obtained for both the temporal frequency shifts of the GONG++ observations in 2001 and for the FWHM shifts of those same observations. Specifically, we show in Figure 3a the frequency dependence of the 25 linear regression slopes from our study of the temporal frequency shifts in which differences in the $|B|_{\text{corr}}$ served as the independent variable, while in Figure 3b we show the frequency dependence of the 25 linear regression slopes from our study of the width shifts using the same independent variable. In both panels we have marked the frequencies where the regression slopes change sign with dashed vertical lines. It is obvious that both the \pm and the \mp zero-crossing frequencies are smaller for the width shifts than they are for the frequency shifts. In Figure 3c we show the dependence of both the \pm and the \mp zero-crossing frequencies upon the mean levels of the International Sunspot Number as computed from our study of the temporal shifts of the p-mode widths. The two solid lines are the linear regression fits to the two sets of zero-crossing frequencies. Both lines have slopes which are similar to, although slightly smaller than, the slopes of the two similar regression lines that we showed in Figure 2 from our analysis of the p-mode frequency shifts.

3. Conclusions

We believe that the changes in the locations of the zero-crossing frequencies can be used as a new tool for probing changes in the sub-surface shear layer since some of the previous theoretical models which have been developed to explain the temporal frequency shifts have found that various combinations of temperature and magnetic field changes can result in a change in the sign of the frequency shifts at high frequencies (Jain & Roberts, 1993; Jain, 1995; Johnston et al., 1995). Hence, we believe that this new observational signature will allow estimates to be made of the changes in both temperature and field strength which occurred between 1996 and 2001. To summarize this important set of results, we have demonstrated

- that the p-mode oscillations demonstrate a complicated pattern in which their frequencies are correlated with changes in solar activity at low frequencies and then become anti-correlated with those changes in activity at intermediate frequencies before once again being positively correlated with the changes in activity at the highest frequencies;
- that the frequencies where the frequency shifts change from being correlated with changes in activity to being anti-correlated with those changes in solar activity (the so-called zero-crossing frequencies) actually change as the mean level of activity changes from month to month and from year to year;
- that the frequencies at which the frequency shifts go back to being positively correlated with the activity changes also changes with the mean level of activity;
- that the frequency dependence of the width shifts is similar to that of the frequencies, but the frequencies at which the sensitivity of the width shifts change from being positive to being negative and vice versa are lower than for the frequencies themselves.

Taken together, all of these new signatures of the temporal shifts in the p-mode frequencies and widths should give the theorists new information to include in their refined models of the causes of these temporal frequency and width shifts.

4. Acknowledgements

In this work we utilized data from the Michelson Doppler Imager (MDI) on the Solar and Heliospheric Observatory (SOHO). SOHO is a project of international cooperation between ESA and NASA. We also utilized data obtained by the Global Oscillation Network Group (GONG) project, managed by the National Solar Observatory, which is operated by AURA, Inc. under a cooperative agreement with the National Science Foundation. The data were acquired by instruments operated by the Big Bear Solar Observatory, High Altitude Observatory, Learmonth Solar Observatory, Udaipur Solar Observatory, Instituto de Astrofísica de Canarias, and Cerro Tololo Interamerican Observatory. The Stanford component of this work was supported by NASA Awards NNX07AK36G and predecessors and NAS5-02139. The portion of this research which was conducted at USC and at the Technical University of Munich was supported by the following grants to USC: NASA Grants NNX08AJ24G, NNX06AC24G, NAG5-13510, NAG5-11582, and NAG5-11001, NSF Grant AST-0307934, and by the following sub-awards from Stanford University to USC: Number 1503169-33789-A and Number 14405890-26967. Some of the computations for this work were carried out at USC using the HPCC and some of them were carried out with the use of the JPL Origin 2000 supercomputers.

5. References

- [1] Jain R 1995 *ESA SP-376* 69
- [2] Jain R and Roberts B 1993 *ApJ* **414** 898
- [3] Johnston A, Roberts B and Wright A N 1995 *ASP Conf. Ser.* **76** 264
- [4] Nigam R and Kosovichev A G 1998 *ApJ* **505** L51
- [5] Rhodes E J Jr, Reiter J, Schou J, Kosovichev A G and Scherrer P H 2001 *ApJ* **561** 1127
- [6] Reiter J, Rhodes E J Jr, Kosovichev A G, Schou J and Scherrer P H 2002 *ESA SP-508* 87